Insight - Civil Engineering 2024, 7(1), 611.
https://doi.org/10.18282/ice.v7i1.611

Article

Fracture mechanism and ductility performances of fiber reinforced shotcrete under flexural loading insights from digital image correlation (DIC)

Tohid Asheghi Mehmandari[1,*], Davood Mohammadi[2], Mohammadreza Ahmadi[1], Mehrdad Mohammadifar[1]

[1] Department of Civil and Environmental Engineering, Amirkabir University of Technology, Iran
[2] Department of Civil Engineering, Islamic Azad University, Central Tehran Branch, Iran
*** Corresponding author:** Tohid Asheghi Mehmandari, T_asheghi@aut.ac.ir, AsheghiTohid@gmail.com

CITATION

Asheghi Mehmandari T, Mohammadi D, Ahmadi M, Mohammadifar M. Fracture mechanism and ductility performances of fiber reinforced shotcrete under flexural loading insights from digital image correlation (DIC). Insight - Civil Engineering. 2024; 7(1): 611. https://doi.org/10.18282/ice.v7i1.611

ARTICLE INFO

Received: 26 April 2024
Accepted: 20 June 2024
Available online: 25 September 2024

Abstract: This paper investigates the fracture mechanism and ductility performance of fiber-reinforced shotcrete (FRS) under flexural loading through digital image correlation (DIC) analysis. The focus is on determining the optimal mix design, utilizing recycled and manufactured fibers in shotcrete through four-point bending tests. These tests reveal significant improvements in flexural strength and ductility, as well as crack resistance, attributed to the synergistic effect of both types of fiber in hybrid fiber reinforcement. Notably, the inclusion of recycled fibers from automobile tires enhances mechanical characteristics and impact resistance, contributing to environmental sustainability and cost reduction. DIC analysis offers crucial insights into crack initiation and propagation in shotcrete, highlighting the impact of fiber reinforcement on crack patterns. Manufactured fibers delay crack onset effectively, while hybridization enhances fracture characteristics, offering improved crack control and flexural strength. The study underscores the potential of hybrid fiber mixes for enhancing structural performance in tunnel support applications, emphasizing the synergistic effect of hybrid of different fiber types. Overall, the research contributes to advancing understanding of fracture behavior in fiber-reinforced shotcrete and provides practical insights for optimizing mix designs to achieve superior mechanical properties and durability.

Keywords: sustainable material; recycled fiber; reinforced shotcrete; digital image process

1. Introduction

Shotcrete is a composite material extensively used in underground structures to strengthen the underlying rock and provide primary support for tunnels. In some cases, with high-quality tunnel surroundings, it can serve as the final lining support. It comprises cement paste, mortar, aggregate, and additives. Two methods are used for its application: the dry-mix and wet-mix systems. Wet-mix shotcrete is more prevalent than dry-mix shotcrete due to its lower risk to human health [1]. Shotcrete, akin to concrete, is susceptible to deterioration and structural failure due to its low tensile strength. Methods such as integrating steel mesh and fibers have been identified to enhance the mechanical properties of plain shotcrete. Steel mesh is widely used as a reinforcement material before the shotcrete process to augment structural integrity and mitigate crack formation in the shotcrete layer [2]. Its ability to be applied easily and effectively on uneven surfaces makes it a favored choice for providing primary support in tunnels [3,4]. Nonetheless, the labor-intensive and time-consuming process of placing steel mesh to prevent cracking poses challenges. These challenges may result in the occurrence of 'shadowing' effects and voids [2,5,6]. In recent years, researchers

have largely advocated for the advantages of substituting or combining regular mesh with fiber reinforcement. Experimental studies have focused on the flexural behavior and failure mechanisms of fiber-reinforced shotcrete [7,8]. Massone and Nazar [9] evaluated the utility of steel or polypropylene fibers in shotcrete as a partial substitute for conventional reinforcement of electro-welded mesh used in subway tunnel support in Santiago. Additionally, Zhu explored the application of a single-layer SFRS and wet-mix technique for permanent tunnel lining, addressing limitations encountered with double-layer linings. The referenced study by Zhu [10] involved laboratory experiments, including compression, tensile, and bending strength tests, on various combinations of steel fibers and other additives, each with different percentages. Various researches were performed to examine the mechanical characteristics of RSF and their potential in structural applications [5,11,12]. In a variety of structural concrete applications, including conventionally placed concrete [13–17], sprayed concrete (shotcrete) [18], self-compacted concrete [5,18,19], and roller-compacted concrete [12,20], it was discovered that RSF can be an ensuring candidate to partially or even completely replace Manufactured steel fibers (MSF). One recent strategy to enhance the mechanical and durability performances of reinforced materials is through the hybridization of various fibers [6,21]. However, most research has focused on hybridization in concrete, overlooking the similar properties of shotcrete and concrete. This strategy can easily be applied to shotcrete as well. Mono fiber reinforcement, where only one type of fiber is incorporated into concrete, is limited in its ability to simultaneously improve both strength and ductility [19,22,23]. For example, adding fibers with high modulus and strength effectively enhances concrete's strength but does not improve its ductility due to their brittle nature. Conversely, incorporating polymeric fibers such as polypropylene significantly enhances ductility, crack resistance, and corrosion resistance [24,25]. Employing hybrid fiber reinforcement, utilizing two or more different types of fibers in concrete, integrates the functionalities of each fiber type to achieve comprehensive enhancements. Among various combinations, steel fiber (SF) and polypropylene fiber (PPF) have emerged as particularly effective in improving the overall properties of the composite, especially in terms of strength and ductility. Numerous studies have investigated the effect of hybrid SF and PPF on the mechanical properties and durability of Fiber Reinforced Concrete (FRC), typically with a total fiber volume fraction (Vf) ranging from 0.5% to 3.6%. For example, research by Yao et al. [26] demonstrated that incorporating hybrid SF and PPF creates a synergistic effect, improving both the strength and ductility of FRC compared to plain concrete mixtures. This finding is supported by studies such as those by de Alencar Monteiro et al. [27] and Li et al. [28], which observed significant enhancements in both peak and post-peak behavior of concrete reinforced with appropriate dosages of SF and PPF. Additionally, including both SF and PPF in concrete helps prevent spalling under fire attack, primarily due to increased permeability [29,30]. Overall, the hybrid effect of combining SF and PPF offers a promising approach to optimize the mechanical properties and durability of FRS and FRC. In fiber reinforced shotcrete, fibers play a critical role in shifting its inherently brittle behavior towards a more ductile response. Acting as structural components, fibers span across cracks, redistributing concentrated tensile stresses that would otherwise lead to cracking [19,30,31]. Consequently, this redistribution fosters a

higher occurrence and dispersion of fractures, thereby enhancing ductility and increasing the presence of smaller cracks throughout the composite [32–34]. The deformation mechanism of fibers relies on their bond with the matrix, which may result in either fiber pull-out or, less frequently, fiber rupture [35]. Achieving a thorough understanding of the flexural behavior of both plain and Fiber Reinforced Shotcrete (FRS) specimens necessitates an examination from a fracture mechanics perspective [36]. Therefore, this study conducted a comprehensive evaluation of shotcrete using a four-point bending test, focusing primarily on fracture mechanics principles. To ensure precise analysis of crack initiation and propagation during testing, Digital Image Correlation (DIC) technology was employed. DIC provides a non-contact, full-field measurement approach, enabling accurate tracking and analysis of surface deformations and crack evolution in brittle materials [37]. Through the acquisition of high-resolution images throughout the flexural test, DIC algorithms effectively correlated displacement and strain fields between successive frames, enabling precise crack detection and monitoring. The incorporation of DIC in this study aims to provide comprehensive insights into reinforced shotcrete, considering mechanical, financial, and environmental factors, particularly through the use of recycled and hybrid fibers.

2. Experimental method

2.1. Material

All shotcrete formulations investigated in this research employed crushed limestone aggregate with a maximum particle size of 9.5 mm, However, due to limitations inherent in laboratory settings, such as the unavailability of spraying equipment, like many researchers, we opted for a shotcrete mix design with limited aggregate size. The cementitious material, as revealed in **Figure 1** through X-ray diffraction (XRD) analysis, remained consistent across all formulations. Enhancements involved the integration of a polycarboxylic ether-based superplasticizer (SP) and an accelerator (AC), provided from S. Shimi Sakhteman. These additives were incorporated at varying proportions, ranging from 0.2% to 2% of the cementitious material's weight for the superplasticizer and from 2% to 5% for the accelerator.

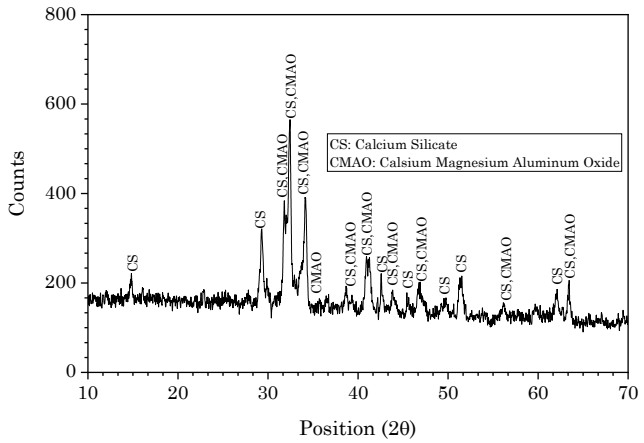

Figure 1. XRD analysis of cement.

Figure 2 displays the raw materials utilized in the shotcrete, highlighting three varieties of fibers: hooked-end manufactured steel fibers, recycled tire steel fibers from Faratav company, and Forta fibers. Detailed properties of these fibers are presented in **Table 1**.

Figure 2. Raw materials of FRS: **(a)** Fine Sand (FS); **(b)** Cement (C); **(c)** Forta Fiber (FF); **(d)** 3D hooked-end Manufactured Steel Fiber (MSF); **(e)** Recycled Steel Fiber (RSF); **(f)** Super Plasticizer (SP).

Table 1. The geometrical and mechanical properties of the fibers.

Type	Length (mm)	Diameter (mm)	Aspect Radio (length/Diameter)	Tensile strength (MPa)	Specific gravity	Elastic modulus (GPa)
MSF	35	0.4	87.5	2830	7.8	210
RSF	20–40	0.35	57–114	3120	6.9	210
FF	60	0.7	85	570–660	0.87	5.5

2.2. Mixing properties

Table 2 delineates the precise mixture compositions for the seven distinct shotcrete mix design scrutinized in this investigation. All mixture design maintained a consistent water-to-binder (w/b) ratio of 0.38. The fiber content for each formulation was standardized at a volume fraction (vf) of 0.3%. This percentage aligns with the recommended range for fiber inclusion in shotcrete applications, as ascertained from comprehensive literature reviews and expert opinions. Within **Table 2**, 'Plain Shotcrete' denotes a mixture devoid of supplementary fibers. The labels 'M', 'R', and 'F' correspond to mix employing solely manufactured steel fiber, recycled steel fiber, and Forta fiber, respectively. The weight proportion of each fiber variant within a mix is delineated in its description. For instance, '0.5MSF-0.5RSF' denotes an equal distribution of 50% for both MSF (Manufactured Steel Fiber) and RSF (Recycled Steel Fiber) within the formulation. For clarity and convenience, each mix design is assigned a symbol in **Table 2**.

Table 2. The mixtures proportions of the plain and FRS mixes.

Mix Description	Symbol	MSF (kg/m^3)	RSF (kg/m^3)	FF (kg/m^3)	Plasticizer (kg/ m^3)
Plain Shotcrete	Plain	0	0	0	0.9
MSF	M	23.49	0	0	1.4
RSF	R	0	20.7	0	1.4
FF	F	0	0	2.61	1.2
0.5MSF-0.5RSF	MR	11.75	10.35	0	1.4
0.5MSF-0.5FF	MF	11.75	0	1.305	1.3
0.33MSF-0.33RSF-0.33FF	MRF	7.752	6.831	0.8613	1.4

In all mixes, 450 kg/m^2 cement, 155 kg/m^2 water, 1695 kg/m^2 aggregate, and 9 kg/m^2 Accelerator (AC) is used. In the preparation of the shotcrete mixtures, cement, fine, and coarse aggregate are initially dry mixed for approximately 2 min. Following this, the SP additive and water were gradually incorporated during mixing for an additional 3 min. Fibers were then introduced to the mixtures, with mixing continuing for a further 3 min. In all Fiber-Reinforced Shotcrete (FRS) variants and the plain shotcrete, an AC was used, constituting 4% of the cement's weight. Subsequent to the mixing process, the fresh shotcrete was poured into beam molds and subjected to external vibration on a shaking table. The samples were demolded after 24 h and then water-cured at a controlled temperature of 20 ± 2 °C for 28 days.

2.3. Test procedure

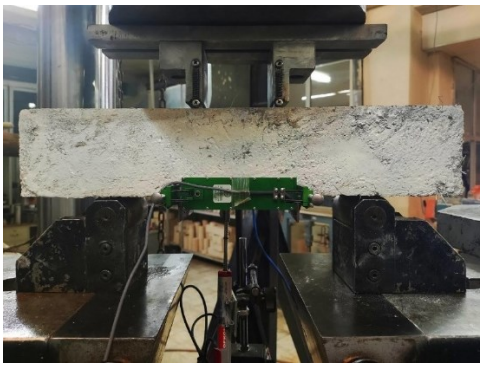

(a)

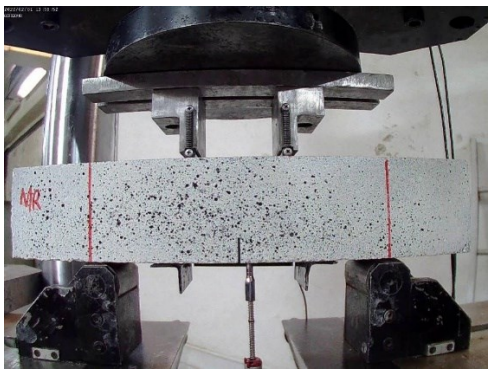

(b)

Figure 3. Four-Point Bending test setup—**(a)** Rear View; **(b)** Front Vie.

Beam specimens measuring 500 mm × 100 mm × 100 mm were prepared for each mix design and underwent flexural strength tests. Each mix design produced three distinct samples. These specimens underwent testing using a four-point bending method, illustrated in **Figure 3**. The choice of the four-point bending test was motivated by its ability to mimic real-world bending forces, which typically concentrate at two points. These tests were conducted under tightly controlled laboratory conditions. To precisely measure beam deflections, a Linear Variable Differential Transformer (LVDT) was positioned at the midspan of each beam. Additionally, an extensometer was utilized to record the Crack Mouth Opening Displacement (CMOD). All tests were executed using Dartec-9600 servo control devices located in the Rock Mechanics Laboratory at Amirkabir University of Technology.

For all the prism samples, the tests for the determination of mechanical and ductility performance of plain and fiber reinforced shotcrete under bending loading were obtained in accordance with the recommendation of RILEM 50-FMC Technical Committee [38]. In order to force the crack to propagate along a desired path, wet sawing was used to notch the prism specimens, which reduced their effective cross sections to 100 × 83 mm. Specimens were rotated over 90° around their longitudinal axes and then sawn through the width of the specimens at mid span. The notched beam specimen and the testing set-up are schematically shown in **Figure 4**.

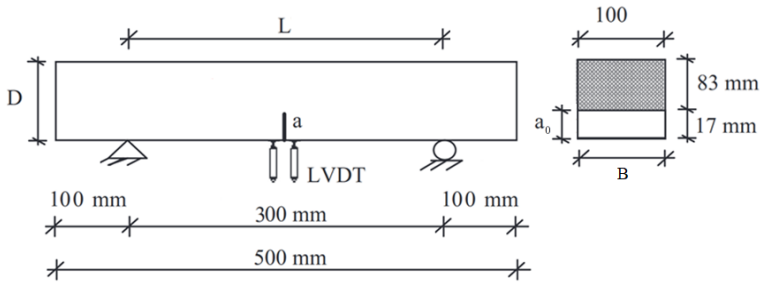

Figure 4. Schematic view of notched sample and test setup.

In this study, load-deflection curves were also used for characterizing the toughness of shotcrete. The area under the load versus deflection at mid span curve is a measure of the fracture energy of the material. Since the fiber reinforced shotcrete have shown a ductile behavior under flexural loads, the tests were finalized when the deflection at midpoint has reached up to 5 mm. The fracture energy was calculated for this deflection based on Equation (1), where G_F: fracture energy (N/m), T_{Total}: area under load versus deflection curve (N.m), m: weight of the specimen (kg), g: gravitational acceleration (9.81 m/s^2), δ_0: deflection of specimen at failure (m), and A_{lig}: effective cross-section of the specimen (m^2). The flexural strength is calculated by using the Equation (2), where F_{net}: flexural strength (MPa), P: maximum load (N), L: span (mm), a_0: notch depth (mm), B: width of the specimen (mm), and D: height of the specimen (mm).

$$G_F = \frac{(T_{Total} + mg\delta_0)}{A_{lig}} \quad (1)$$

$$F_{net} = \frac{PL}{B(D - a_0)^2} \quad (2)$$

The main factor affecting the toughness value is the energy absorbed per unit volume of the specimens, which particularly refers to the region under the load-deflection curve. The first fracture toughness assesses the amount of energy and stress that a specimen can withstand at the point of its first crack formation. Additionally, it demonstrates the specimen's lack of elasticity when subjected to stress until it ultimately fails due to bending. The toughness capabilities of plain shotcrete and FRS specimens are determined in this research by calculating the regions under their load-deflection curves. The technique used to compute the values of T_{pre} and T_{post} toughness is as follows. T_{pre} refers to the integral of the load-deflection curve of the specimen, namely the region between the initial point of the curve and the point of maximum load. Conversely, T_{post} refers to the region under the load-deflection curve of the specimen, namely between the highest load point and the deflection of 5 mm. The two parameters provide a more profound understanding of how the fibers contribute to the behavior of the elastic and inelastic sections of the specimens. **Figure 5** shows T_{pre}, T_{post}, and the sum of these two toughness values, T_{Total}, schematically.

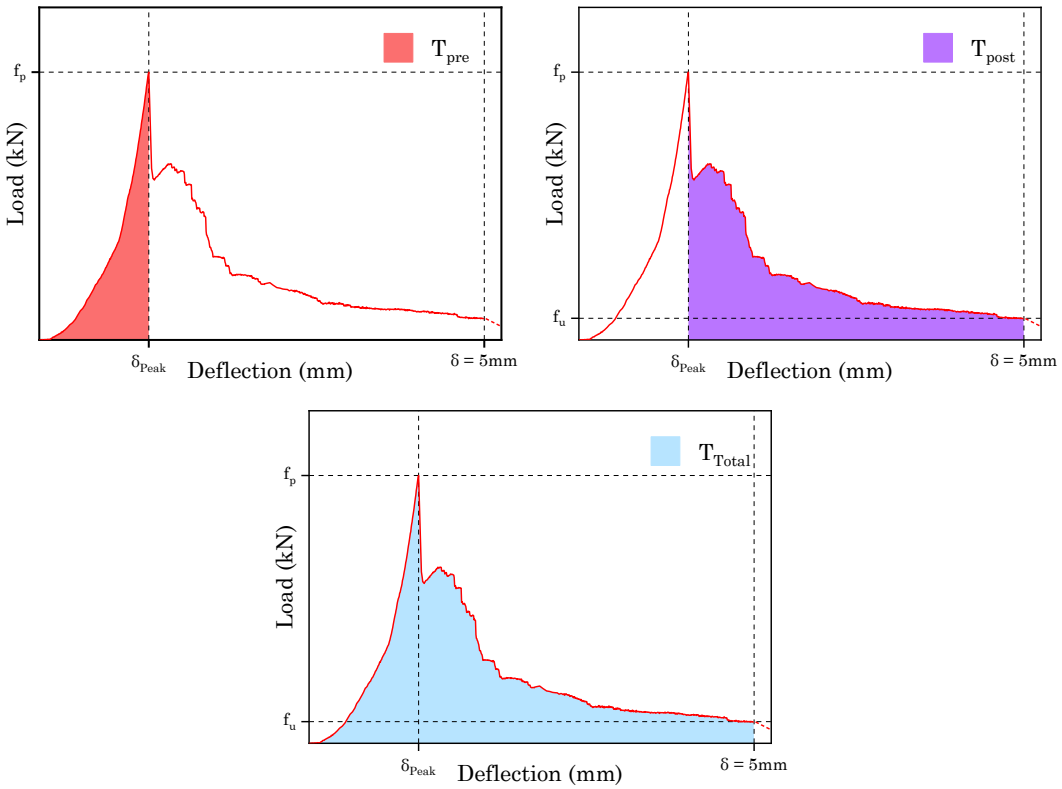

Figure 5. Schematic illustration of Toughness: T_{pre}, T_{post}, and T_{Total} analysis.

2.4. DIC measurement

To monitor the creation and spread of fractures and back-calculate the strain distribution throughout the material, Digital Image Correlation (DIC), an optical, high-precision, non-contact measuring method, was used. Specific sample preparation procedures were used to generate high-quality digital pictures and accurate findings. The cross-section of the four-point flexural test material was randomly marked with

contrasting black and white sections to improve visibility and enable observation. Furthermore, random parts of compression and stress specimens are sprayed. To minimize distractions, a professional digital camera with a 1/2.8″ 3M Sony IMX036 CMOS sensor was mounted on a strong tripod, and video recording started concurrently with the test, capturing the whole loading procedure. Tests Setup and DIC equipment illustrated in **Figure 6**, were employed to guarantee constant light contrast. The video was captured at the start of the loading and edited using Aoao software after it finished. 280 images are collected from each movie, in order to perform image analysis. To quantify the strain distribution and explore the development and propagation of fractures, the generated digital pictures were processed using Ncorr, a free, high-quality, and adaptable DIC program. Further validation using traditional measurement methods that depend on physical touch was deemed necessary to corroborate the correctness of the strain distribution data produced by DIC. To properly monitor vertical and horizontal displacements, an LVDT and an EXTENSOMETER were utilized.

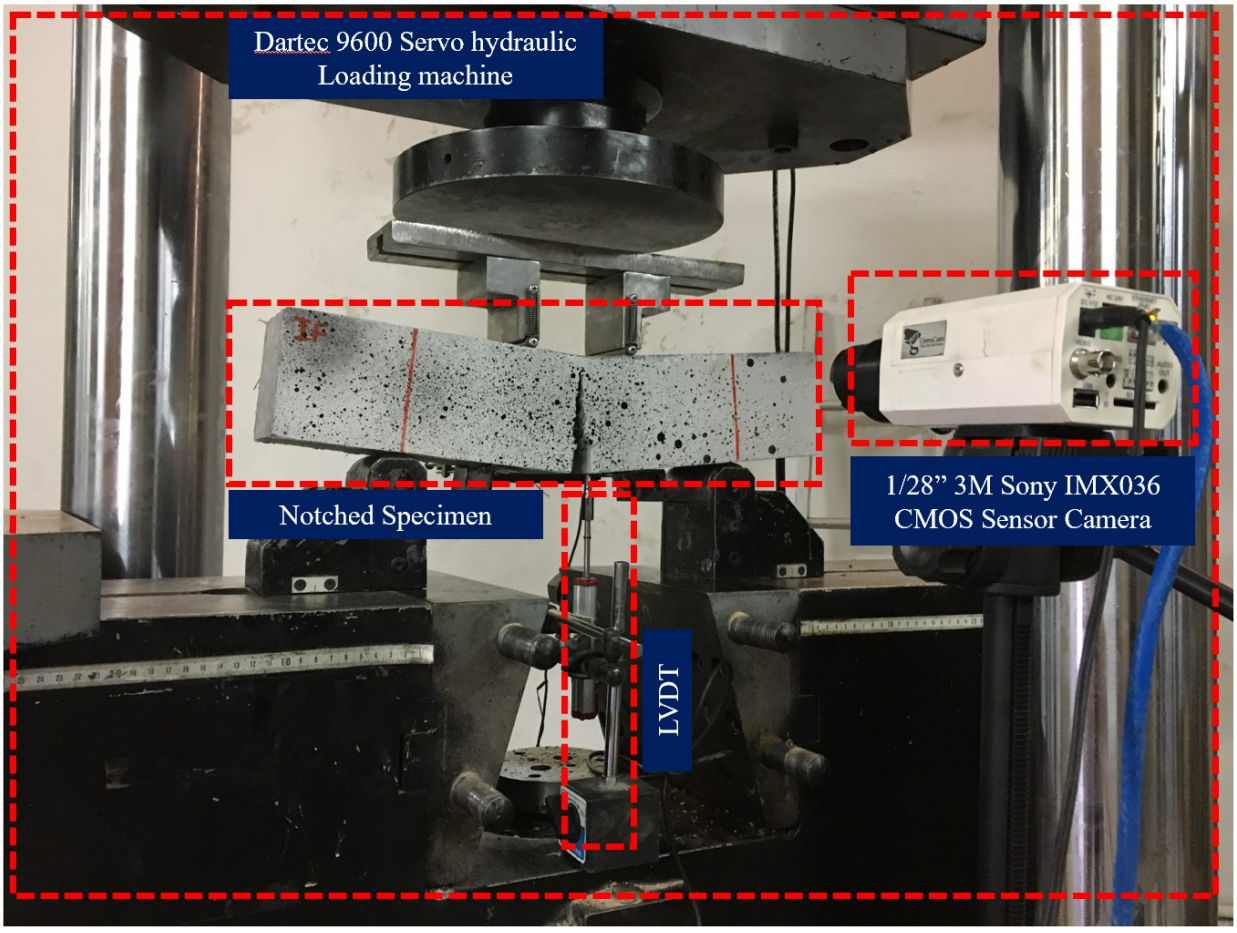

Figure 6. Tests setup and DIC equipment.

3. Experimental results and discussion

3.1. Flexural performance

The study compared the flexural behavior of fiber-reinforced shotcrete (FRS) and plain shotcrete (PS) using experimental results. The results showed that PS samples

showed brittle characteristics, with a sharp decline in stress post-peak and lower deflection at maximum stress compared to FRS samples. However, all FRS samples showed increased ductility, allowing further loading post-peak. This enhanced ductility can be attributed to fiber inclusion, which acts as crack regulators and improves energy absorption during deformation. FRS samples also displayed exceptional performance post-peak, with significantly higher peak strain values, indicating the significant influence of fibers in delaying crack initiation and reaching maximum strain. FRS samples displayed three distinct characteristics after the peak: PS samples lack post-peak behavior, while PS samples show a pronounced peak followed by a gradual decline, indicating significant energy absorption. Samples R, F, MR, and MRF displayed a sharp stress drop post-peak, followed by a steady decline until rupture. Sample MF displayed hybrid behavior, with an initial peak followed by a marked decrease, then a gradual rise in the flexural curve. Flexural stress-displacement curves for all plain and fiber reinforced shotcrete samples are shown in **Figure 7**.

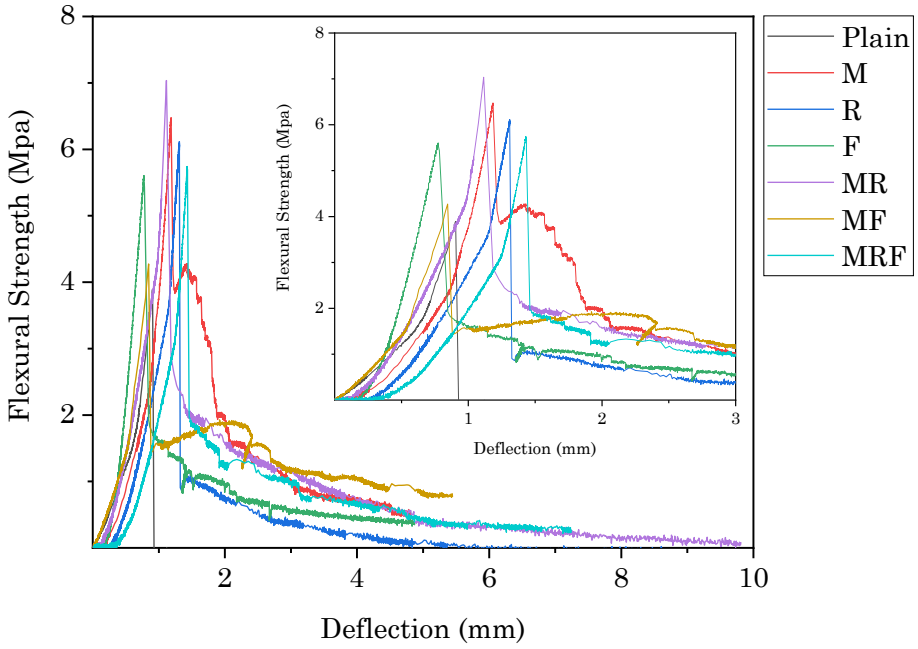

Figure 7. Flexural stress-displacement curves for all plain and fiber reinforced shotcrete samples.

3.2. Hybridization effect of FRS manufactured on flexural Toughness and flexural Fracture Energy

Table 3 shows computed values for toughness and fracture energy, highlighting the impact of fiber reinforcement on flexural toughness. **Figure 8** illustrates the toughness values, T_{pre} and T_{post}, for both plain and FRS samples. All FRS samples display enhanced energy absorption, with minimal T_{post} values. The PS sample's toughness is limited to its elastic behavior (T_{pre}), which is directly proportional to peak strength and deflection in all samples. Steel fibers in single-fiber mixes demonstrate superior T_{pre} values, enhancing pre-peak ductility and delaying crack onset compared to forta fibers. The MR specimen shows exceptional pre-peak energy absorption, while

the MRF mix also performs well in this aspect. However, adding forta fibers is less favorable due to environmental and economic concerns and their lower toughness compared to the MR sample.

Table 3. Toughness and Fracture energy result of plain and FRS specimens obtained from experimental results.

Mix description	Toughness results			Fracture energy result				
	T_{pre} (N.m)	T_{post} (N.m)	T_{total} (N.m)	T_0 (N/m)	m (N.m)	Delta0 (N.m)	A_{lig} (N.m)	G_f (N.m)
Plain	2.874	0.000	2.874	2.874	11.51	0.00093	0.0083	358.942
M	4.764	12.514	17.278	17.278	11.68	0.00481	0.0083	2148.053
R	4.853	3.639	8.492	8.492	11.44	0.005	0.0083	1090.778
F	3.053	7.559	10.612	10.612	10.67	0.004869	0.0083	1340.002
MR	5.298	10.992	16.290	16.290	12.19	0.005	0.0083	2034.648
MF	2.884	12.838	15.722	15.722	11.97	0.005	0.0083	1965.003
MRF	4.472	7.963	12.435	12.435	11.76	0.005	0.0083	1567.694

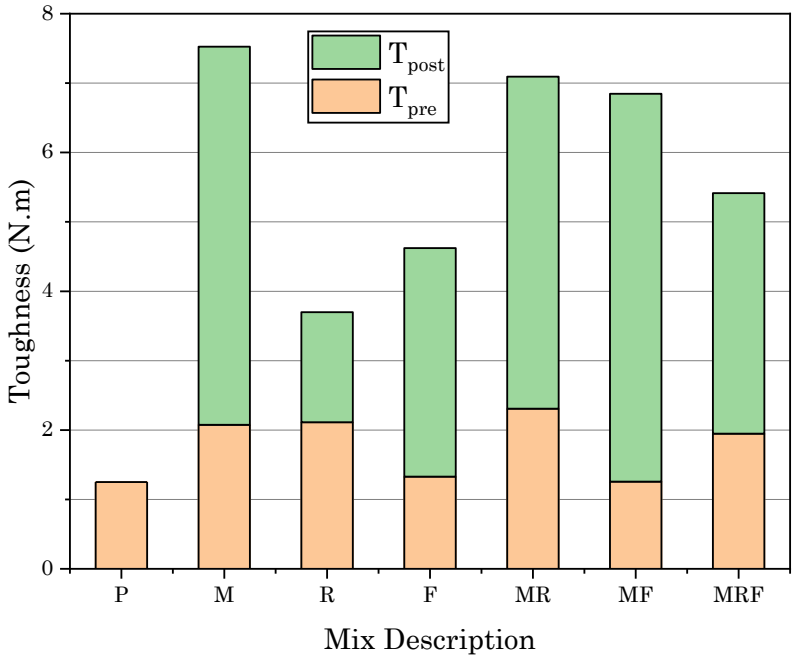

Figure 8. Toughness values of plain and FRS specimens obtained from experimental results.

T_{post} values from the R sample confirm the limitations of recycled fibers in post-peak zone. While forta fibers improve energy absorption to some extent, the disparity in T_{post} values between the M sample and other single-fiber mixes highlights the effectiveness of the hooked ends in manufactured fibers. These hooks interlock with the shotcrete matrix, transmitting stress across cracks similarly to rebar reinforcement. Hybrid mixes using MSFs, like the MR mix, show increased T_{post} values. The MR mix outperforms the M sample, using fewer manufactured fibers. Given the environmental and economic benefits of RSF and the MF sample's limited pre-peak energy absorption, the MR mixture is considered the most optimal in terms of toughness.

Figure 9 presents the calculated fracture energy values. These values are crucial for understanding the FRS's ability to slow down crack propagation, taking into

account the sample's weight. Plain shotcrete shows the lowest fracture energy, highlighting its brittleness in flexural tests. The M sample has the highest fracture energy at 2148 N/m, with the R and F single-fiber samples recording 1091 N/m and 1340 N/m, respectively. Hybrid samples, however, exhibit higher G_f values than these single-fiber samples, despite having the same fiber volume fraction.

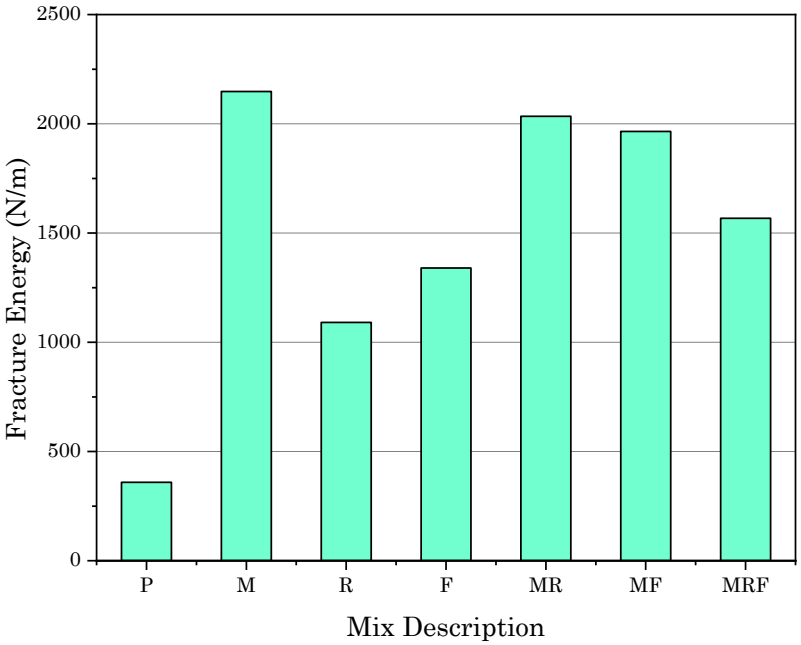

Figure 9. Fracture energy results of plain and FRS specimens obtained from experimental results.

Both forta and manufactured fibers effectively enhance the shotcrete's post-peak behavior. The MF sample, a hybrid, has a slightly lower fracture energy than the M sample, indicating that hybridization didn't significantly boost energy absorption. Comparing the MRF with the MR mix, adding forta fibers to the MR mix doesn't increase its G_f. Thus, the MR hybrid is the most effective among the hybrids. The G_f value in the MR sample shows a minor 5% decrease due to the hybridization of MSF with RSF. With the environmental and economic advantages of RSFs, the MR hybrid emerges as a more beneficial choice than the M single-fiber mix.

3.3. Analysis of cracks and localized damage using DIC

Examining crack characteristics, such as crack width and crack length, in shotcrete material components is essential [39,40]. DIC analysis can provide valuable assistance in this matter. Cracks observed on the surface of a shotcrete element are indicative of the internal propagation of cracks within the element. Furthermore, the examination of crack patterns can provide crucial insights on the distribution of stress within structural components. Additionally, the reinforcement characteristics of FRS elements can have an impact on the development and formation of cracks. This section will assess crack initiation and crack propagation patterns as indicators that represent the extent of damage on the surface. Crack patterns pertain to the geometric characteristics and orientation of the crack. Cracks can vary in orientation, either diagonal or parallel to the direction of the loading, and can have varying widths and

heights. However, in this case the presence of a notch in the bottom of samples restricts the direction of cracks to vertical cracks. The color scale employed for DIC analysed images represents the magnitude of horizontal displacement in millimetres at any given position inside the sample. The blue sections exhibit the least amount of lateral displacement, whilst the brown sections display the highest degree. **Table 4** encounters 8 processed images from each of the 7 specimens of the test. Render analysed using Ncorr software [39,40], the process of crack initiation and its propagation is examined from the start of the loading phase up till the deflection point of 5 mm. These photos illustrate the gradual deterioration of the surface that occurred on each sample. **Figure 10** depicts the DIC analysis in conjunction with the flexural stress-deflection curve of the M sample, providing a vivid depiction of the formation and propagation of cracks during the test.

Table 4. DIC analysis results.

#	a = 0 mm	b = 1 mm	c = 1.5 mm	d = 2 mm	e = 2.5 mm	f = 3 mm	g = 4 mm	h = 5 mm	Scale
Plain	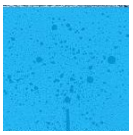	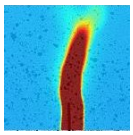							
M	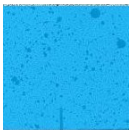	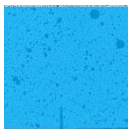	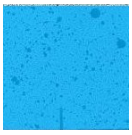	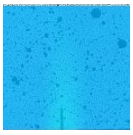	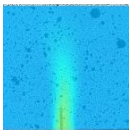	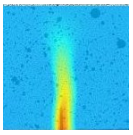	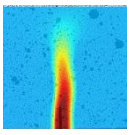	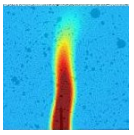	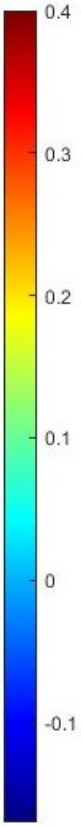
R	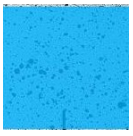	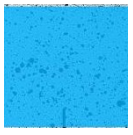	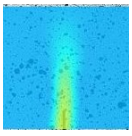	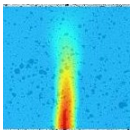	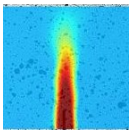	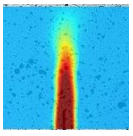	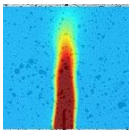	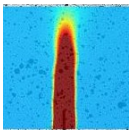	
F		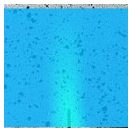	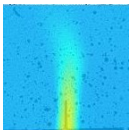	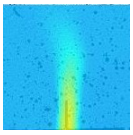	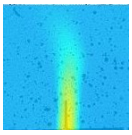	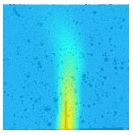	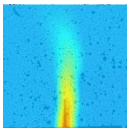	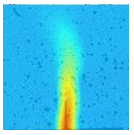	
MR			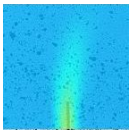	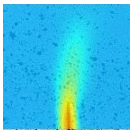	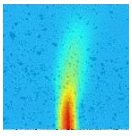	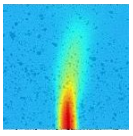	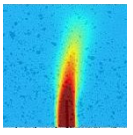	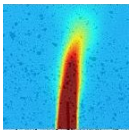	
MF	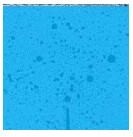	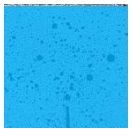	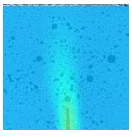	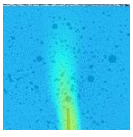	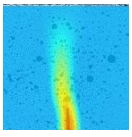				
MRF									

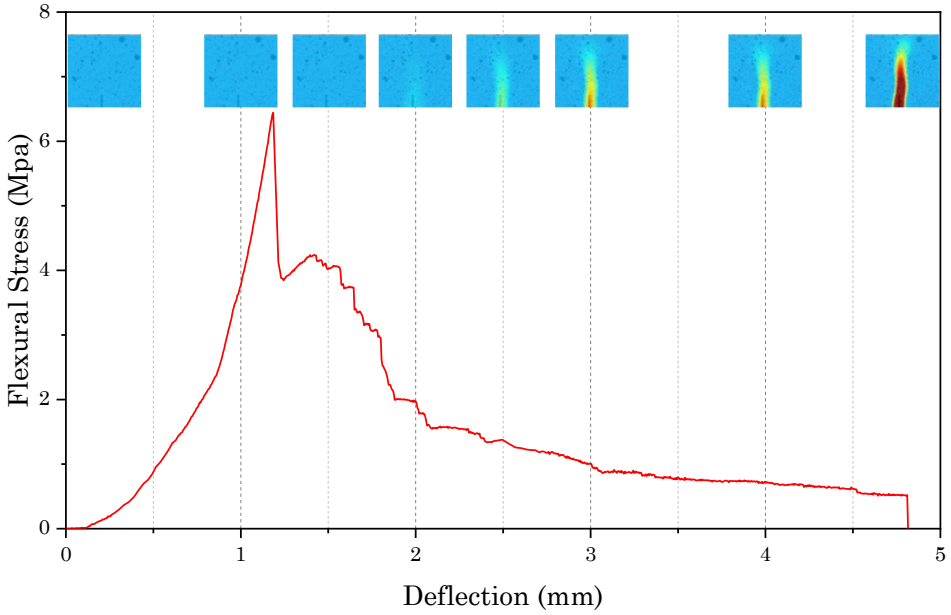

Figure 10. DIC analysis in conjunction with the flexural stress-deflection curve of the M sample.

There is a noticeable delay in the DIC images when compared to the flexural stress-deflection curves. For example, there are 6 samples in stage (b) that have an undamaged surface. According to **Table 4**, samples with deflection values near 1 mm will likely develop cracks, given their maximum strength deflection. In fact, crack initiation takes place within the sample, and as it develops, the fractures eventually reach the surface of the sample, becoming visible for DIC examination. Consequently, since the cracks are extending towards the surface, there is no noticeable alteration in the DIC analysis. This causes a delay in analysing surface cracks compared to the initial formation of cracks in the specimen.

The DIC analysis shown in **Table 4** provides clear evidence of the brittle nature of PS during the four-point flexural test. The plain shotcrete sample experiences full failure under flexural loading, failing to reach a deflection of 1 mm. The failure of the PS sample is significantly more abrupt compared to all other shotcrete samples, as evident from the FRS photos in stage (b). Hence, the inclusion of fiber reinforcement effectively delays the occurrence of the peak point, while also offering post-peak behavior for the shotcrete sample.

According to **Table 4**, the M sample represents the most effective mixture in delaying the initiation of cracks among single-fiber mixes. While the M sample reaches its peak flexural strength at a deflection of 1.185 mm, there is no indication of surface deformation until step (d). This characteristic is mainly advantageous for controlling the propagation of cracks during the initial stages of post-peak behavior, since it assesses the distribution of stress in the fiber after reaching its peak. Furthermore, it is advantageous for the element's serviceability to have an undamaged surface throughout the initial stages after reaching its maximum stress. Furthermore, the progressive development of crack length and width from stages (c) to (f) indicates that most of the manufactured fibers have successfully formed a strong bond with the shotcrete matrix prior to become dependent on their hooked-ends. Nevertheless, the

notable rise in crack width during phases (g) and (h) suggests that most manufactured fibers ultimately undergo fiber pullout in their straight length, resulting in the interlocking of their hooked-ends with the shotcrete matrix.

Upon comparing the analysed photos of the R sample with the M sample, it is apparent that the R sample is less effective in delaying the initial appearance of cracks. Furthermore, the crack length in stage (c) is almost equivalent to the length in stage (h). From stages (c) to (h), the only thing that increases is the severity of the damaged area, which is directly related to the length of the main crack. This occurrence is distinct from the gradual formation of cracks on the surface of the M sample. What happened, took place due to the notably smaller thicknesses and dimensions of recycled fibers. Once the crack length gets higher than a specific threshold, the ability of RSFs to bridge the crack diminishes, resulting in the pullout of the fibers. Sample R exhibits a greater crack width during the test compared to sample M due to the same incident mentioned.

The analysis of the processed pictures obtained from the F sample provides evidence that the utilization of forta fibers as single-fiber reinforcement leads to a reduction in the pre-peak ductility of the shotcrete sample. As demonstrated in step (b), the F sample exhibits surface damage earlier than the plain sample. This implies that this mix accelerates the attainment of the peak flexural strength in shotcrete. However, the behavior of the F sample after reaching its peak differs when compared to single-fiber steel reinforcement. During stages (c) to (h), the increase in crack width and length is significantly less pronounced compared to the M and R samples. The behavior is a result of the inherent characteristics of forta fibers. The analysis of processed images suggests that forta fibers exhibit satisfactory performance in terms of forming a strong bond with the shotcrete matrix. Nevertheless, the notably low modulus of elasticity and generally weak mechanical properties of the material lead to fiber rupture when subjected to the flexural test. Thus, the crack width is consistently regulated by the crack bridging of forta fibers, while the flexural stress in the specimen remains low due to the sample's limited flexural capacity.

When comparing hybrid samples in relation to crack patterns, it is advisable to assess them by considering the results from the single-fiber samples as well. The DIC results of the MR sample indicate that hybridization has a favorable impact on improving fracture characteristics. The crack width and length are both reduced compared to the R sample. In addition, the MR sample effectively controlled the crack length to a similar extent as the M sample, while utilizing approximately half of the MSFs employed in the M mix design. The observed trendline in MR images aligns with the trendline in the M sample, suggesting that this sample experiences a synergistic impact from hybridization. Furthermore, the shotcrete specimen in the mid-span section of the MR sample. Evidently, the increased depth of the section results in an enhanced flexural strength of the sample. The hybridization of FF with MSF, as indicated by the DIC analysis in **Table 4** does not lead to improved crack characteristics. The crack width and crack length in the MF samples are found to be higher when compared to the M and F samples. The intensity of surface damage is further heightened in the later phases. Yet, the degree of cracking is still lower in comparison to MR hybrid samples, before reaching stage (f). In fact, DIC analysis shows that MF hybrid mix has enhanced only in the first half of the post-peak zone,

which was evident in **Figure 7**. Nevertheless, it is clear that forta fiber is ineffective in regulating the crack width in MF mix, unlike in F mixture.

The hybridization of three types of fiber did not yield superior results when compared to the MR sample. The magnitude of surface damage is markedly amplified from stage (d) to the endpoint of the test. The presence of FF is inefficient in controlling crack width, as seen by the increased crack width. Indeed, the MRF hybrid sample may exhibit heterogeneous behavior due to the presence of several fiber types inside the shotcrete matrix. The primary objective of hybridization is to capitalize on the favorable attributes of each fiber type. However, the inclusion of forta fibers in the MRF sample appears to just diminish the specimen's ability to resist fracture. Furthermore, the inclusion of FFs may have resulted in an interference with the performance of RSFs and MSFs, as the MRF sample experiences considerable crack width in the initial phases of the post-peak zone. However, the limited fiber content in each fiber type can make the fiber reinforcing ineffective. Nevertheless, the MRF mixture fails to achieve superior results in mitigating crack formation.

4. Conclusion

1) Bending performance: FRS exhibited notably superior ductility and strength compared to PS, evidenced by increased peak strain values and more pronounced deflections under peak loads.
2) Fracture Energy: the analysis of fracture energy in fiber-reinforced shotcrete (FRS) demonstrates enhanced flexural toughness, particularly in hybrid mixes like MR, which optimize both environmental and economic factors. Manufactured fibers prove effective in pre-peak energy absorption, while the MR hybrid emerges as the most beneficial choice, offering a minor decrease in G_f value compared to single-fiber mixes.
3) Localized damage: DIC analysis offers crucial insights into crack initiation and propagation in shotcrete, highlighting the impact of fiber reinforcement on crack patterns. Single-fiber mixes exhibit distinct behaviors, with manufactured fibers delaying crack onset effectively. Hybridization, particularly in MR samples, enhances fracture characteristics, offering improved crack control and flexural strength. However, hybridization with forta fibers in MF and MRF samples shows limited effectiveness, indicating a need for careful consideration of fiber types in shotcrete reinforcement strategies.
4) Fiber Types Analysis: Distinct behaviors were observed for different fiber types. Manufactured fibers showed notable peaks and gradual decreases in flexural curves, indicating effective energy absorption and interlocking. Recycled fibers exhibited smoother post-peak curves, suggesting stronger bonding and pullout resistance.
5) Hybridization Effect: The combination of recycled and manufactured fibers in the hybrid mix resulted in a remarkable 80.9% boost in peak flexural strength compared to plain shotcrete. This significant improvement emphasizes the synergistic effect of blending different fiber types, substantially enhancing both flexural strength and resistance to crack formation in shotcrete. This discovery underscores the potential of hybrid fiber mixes for enhancing structural

performance in tunnel support applications.

Author contributions: Conceptualization, TAM and MM; methodology, DM; software, DM and TAM; validation, MA, MM and TAM; formal analysis, MA; investigation, MA; resources, DM; data curation, TAM; writing—original draft preparation, MA and TAM; writing—review and editing, TAM and MA; visualization, MA; supervision, TAM; project administration, TAM. All authors have read and agreed to the published version of the manuscript.

Conflict of interest: The authors declare no conflict of interest.

References

1. Franzén T. Shotcrete for underground support: a state-of-the-art report with focus on steel-fibre reinforcement. Tunnelling and Underground Space Technology. 1992; 7(4): 383-391. doi: 10.1016/0886-7798(92)90068-S
2. Sun PP, Yang XX, Qiao WG, et al. Optimally designed shotcrete material and its cooperating performance when integrated with sandstone. Construction and Building Materials. 2020; 249: 118742. doi: 10.1016/j.conbuildmat.2020.118742
3. Mohammadifar M, Asheghi Mehmandari T, Fahimifar A. Parametric and Sensitivity Analysis on the Effects of Geotechnical Parameters on Tunnel Lining in Soil Surrounding. Journal of Structural and Construction Engineering. 2024. doi: 10.22065/JSCE.2024.422469.3250
4. Asheghi Mehmandari, T., Engineering Concept and Construction Methods of High-Rise Building. Vol. 4. 2023, Iran: Sanei 308.
5. Hossain MS, Han S, Kim SK, et al. Long-term effect of accelerator content on flexural toughness of steel fiber reinforced shotcrete for tunnel construction. Case Studies in Construction Materials. 2021; 15: e00706. doi: 10.1016/j.cscm.2021.e00706
6. Mehmandari TA, Shokouhian M, Imani M, Fahimifar A. Experimental and numerical analysis of tunnel primary support using recycled, and hybrid fiber reinforced shotcrete. Structures. 2024; 63: 106282. doi.org/10.1016/j.istruc.2024.106282
7. Adegoke M, Shokouhian M, Ntonifor C. AFRP Reinforced Concrete Column with Controlled Rocking Connection. Structures Congress 2022. Published online April 18, 2022. doi: 10.1061/9780784484180.010
8. Farokhi Zadeh S, Moradi M, Hojatkashani A. Evaluating the Effect of Fiber Addition on Seismic Performance of Segmental Tunnel Lining. International Journal of Advanced Structural Engineering. 2022; 12(4).
9. Massone LM, Nazar F. Analytical and experimental evaluation of the use of fibers as partial reinforcement in shotcrete for tunnels in Chile. Tunnelling and Underground Space Technology. 2018; 77: 13-25. doi: 10.1016/j.tust.2018.03.027
10. Zhu Y. Study on Mechanical Characteristics of Steel Fiber Reinforced Shotcrete and Its Application in Single Layer Tunnel Lining. Chongqing University; 2009.
11. Ahmad S, Sharif AMA, Al-Osta MA, et al. Flexural performance of pre-damaged RC beams strengthened with different configurations of UHPFRC layer –experimental and analytical investigation. Structures. 2023; 48: 1772-1787. doi: 10.1016/j.istruc.2023.01.077
12. Angelakopoulos H. Reused Post-consumrer Tyre Steel Fibres in Roller Compacted Concrete. University of Sheffield; 2016.
13. Mostafa OM, Rahman MK, Al-Zahrani MM, et al. Flexural behavior and bond coefficient of BFRP bar reinforced normal and high strength concrete beams. Construction and Building Materials. 2023; 401: 132896. doi: 10.1016/j.conbuildmat.2023.132896
14. Younis KH, Pilakoutas K. Strength prediction model and methods for improving recycled aggregate concrete. Construction and Building Materials. 2013; 49: 688-701. doi: 10.1016/j.conbuildmat.2013.09.003
15. Jafarifar N. Shrinkage behaviour of steel-fibre-reinforced-concrete pavements. University of Sheffield; 2012.
16. Hu H, Papastergiou P, Angelakopoulos H, et al. Mechanical properties of SFRC using blended manufactured and recycled tyre steel fibres. Construction and Building Materials. 2018; 163: 376-389. doi: 10.1016/j.conbuildmat.2017.12.116
17. Bjegovic D, Baricevic A, Lakusic S, et al. Positive interaction of industrial and recycled steel fibres in fibre reinforced concrete. Journal of Civil Engineering and Management. 2014; 19(Supplement_1): S50-S60. doi: 10.3846/13923730.2013.802710

18. Groli G, Pérez Caldentey A, Soto AG. Cracking performance of SCC reinforced with recycled fibres – an experimental study. Structural Concrete. 2014; 15(2): 136-153. doi: 10.1002/suco.201300008
19. Nematian Jelodar H, Hojatkashani A, Madandoust R, et al. Experimental study of fiber concrete slab behavior against high electric heat. International Journal of Advanced Structural Engineering. 2023; 13(1).
20. Neocleous K, Angelakopoulos H, Pilakoutas K, et al. Fibre-reinforced roller-compacted concrete transport pavements. Proceedings of the Institution of Civil Engineers - Transport. 2011; 164(2): 97-109. doi: 10.1680/tran.9.00043
21. Fahimi E, Ahmadi M. Investigation of Lateral Load Capacity of Rectangular Reinforced Concrete Columns Strengthened with GFRP Bars Wrapped with CFRP Helices. SSRN Electronic Journal. Published online 2023. doi: 10.2139/ssrn.4454609
22. Pakravan HR, Latifi M, Jamshidi M. Hybrid short fiber reinforcement system in concrete: A review. Construction and Building Materials. 2017; 142: 280-294. doi: 10.1016/j.conbuildmat.2017.03.059
23. Ramezanianpour AA, Kazemian M, Sedighi S, et al. Study durability of mortars with natural pozzolans under carbonation. New Approaches in Civil Engineering. 2019; 3(2): 63-75.
24. Pakravan HR, Ozbakkaloglu T. Synthetic fibers for cementitious composites: A critical and in-depth review of recent advances. Construction and Building Materials. 2019; 207: 491-518. doi: 10.1016/j.conbuildmat.2019.02.078
25. Kazemian M, Sedighi S, Ramezanianpour AA, et al. Effects of cyclic carbonation and chloride ingress on durability properties of mortars containing Trass and Pumice natural pozzolans. Structural Concrete. 2021; 22(5): 2704-2719. doi: 10.1002/suco.201900529
26. Yao W, Li J, Wu K. Mechanical properties of hybrid fiber-reinforced concrete at low fiber volume fraction. Cement and concrete research. 2003; 33(1): 27-30. doi: 10.1016/S0008-8846(02)00913-4
27. de Alencar Monteiro VM, Lima LR, de Andrade Silva F. On the mechanical behavior of polypropylene, steel and hybrid fiber reinforced self-consolidating concrete. Construction and Building Materials. 2018; 188: 280-291. doi: 10.1016/j.conbuildmat.2018.08.103
28. Li B, Chi Y, Xu L, et al. Experimental investigation on the flexural behavior of steel-polypropylene hybrid fiber reinforced concrete. Construction and Building Materials. 2018; 191: 80-94. doi: 10.1016/j.conbuildmat.2018.09.202
29. Li Y, Pimienta P, Pinoteau N, et al. Effect of aggregate size and inclusion of polypropylene and steel fibers on explosive spalling and pore pressure in ultra-high-performance concrete (UHPC) at elevated temperature. Cement and Concrete Composites. 2019; 99: 62-71. doi: 10.1016/j.cemconcomp.2019.02.016
30. Zare P, Asheghi T, Fahimifar A, Zabetian S. Experimental Assessment of Damage and Crack Propagation Mechanism in Heterogeneous Rocks. In: Proceedings of 5th International Conference on Applied Research in Science and Engineering; July 2020; Amsterdam, Netherlands.
31. Moghadasi H, Eslami A, Akbarimehr D, Afshar D. Numerical Investigation of Adjacent Construction Considering Induced Instability. Transportation Infrastructure Geotechnology. 2024; 11: 1143-1167. doi: 10.1007/s40515-023-00319-w
32. Asheghi Mehmandari T, Fahimifar A, Asemi F. The Effect of the Crack Initiation and Propagation on the P-Wave Velocity of Limestone and Plaster Subjected to Compressive Loading. AUT Journal of Civil Engineering. 2020; 4(1), 55-62. doi: 10.22060/AJCE.2019.15984.5558
33. Eslami A, Afshar D, Moghadasi H, Akbarimehr D. Numerical and Experimental Investigations of Interference Effect of Adjacent Buildings on Sand and Fill Deposits. International Journal of Civil Engineering. 2024; 22, 723-738. doi: 10.1007/s40999-023-00907-4
34. Ramezanian AA, Sedighi S, Kazemian M, Ramezanianpour AM. Effect of micro silica and slag on the durability properties of mortars against accelerated carbonation and chloride ions attack. AUT Journal of Civil Engineering. 2020; 4(4): 411-422. doi: 10.22060/ajce.2020.15943.5565
35. Zacharda V, Němeček J, Štemberk P. Micromechanical performance of interfacial transition zone in fiber-reinforced cement matrix. IOP Conference Series: Materials Science and Engineering. 2017; 246: 012018. doi: 10.1088/1757-899x/246/1/012018
36. Ntonifor CN, Shokouhian M, Adegoke M. Investigation of the Rotation Capacity and Flexural Strength of Web Tapered Hybrid High Strength Steel Simple Supported I-Section. Structures Congress 2022. Published online April 18, 2022. doi: 10.1061/9780784484180.009
37. Ündül Ö, Amann F, Aysal N, et al. Micro-textural effects on crack initiation and crack propagation of andesitic rocks. Engineering Geology. 2015; 193: 267-275. doi: 10.1016/j.enggeo.2015.04.024

38. Recommendation, R.D. Determination of the fracture energy of mortar and concrete by means of three-point bend tests on notched beams. Materials and Structures. 1985; 18(4): 287-290. doi: 10.1007/bf02472918
39. Harilal R, Ramji M. Adaptation of open source 2D DIC software Ncorr for solid mechanics applications. In: Proceedings of 9th International Symposium on Advanced Science and Technology in Experimental Mechanics, 1-6 November, 2014, New Delhi, India.
40. Ncorr version 1.2. Available online: https://www.ncorr.com/index.php/downloads (accessed on 17 January 2018).